Chalcogenide Letters Vol. 13, No. 5, May 2016, p. 187 - 199

ELECTROCHEMICAL DEPOSITION OF ZINC TELLURIDE THIN FILMS FROM ETHALINE IONIC LIQUID

A. S. CATRANGIU[a], M. BEREGOI[b], A. COJOCARU[a*], L. ANICAI[c], A. COTARTA[a], T. VISAN[a]

[a]*Department of Inorganic Chemistry, Physical Chemistry and Electrochemistry, University POLITEHNICA Bucharest, Calea Grivitei 132, 010636 Bucharest, Romania*

[b]*National Institute of Materials Physics, Atomistilor 105 bis, 077125 Magurele, Ilfov, Romania*

[c]*Center of Surface Science and Nanotechnology, University POLITEHNICA Bucharest, Splaiul Independentei 313, 060042 Bucharest, Romania*

The electrochemical deposition of Zn_xTe_y thin films was studied in an ionic liquid consisted in choline chloride - ethylene glycol eutectic mixture (Ethaline). $ZnCl_2$ and TeO_2 precursors were dissolved in 5-24 millimolar concentrations and the temperature was maintained constant at 60 ^oC. Cyclic voltammograms on Pt from electrolytes with both Te^{4+} and Zn^{2+} ions displayed three cathodic processes as limiting currents or peaks: Te underpotential deposition, codeposition of ZnTe compound, and deposition of Zn-rich binary telluride. The corresponding anodic waves or peaks were also identified. The shape of Nyquist electrochemical impedance plots recorded on various applied polarization showed that the electrode first covers with a Te film, and then the more cathodic polarization produces a co-reduction of Te^{4+} with Zn^{2+} as ZnTe compound. The formation of Zn metal-rich Zn_xTe_y film at excessive negative polarization is indicated by the lowest value of maximum phase angle in Bode plots. The Zn/Te ratio (apparent stoichiometry) in the films deposited on Cu substrate is controlled by carrying out constant potential electrolyses with different ionic ratios in Ethaline bath. Film morphology, elemental analysis, and crystalline structure were evidenced by SEM microscopy, EDX analysis and X-ray diffraction, respectively.

(Received January 27, 2016; Accepted May 2, 2016)

Keywords: Electrochemical deposition, Zinc telluride film, Ethaline, Morphology, Crystalline structure

1. Introduction

Zinc telluride, ZnTe, is a binary semiconductor compound [1,2] with a large and direct energy gap, 2.25-2.26 eV, at room temperature. Its wide range of potential applications in thermoelectricity, optoelectronic materials, photoelectrodes in solar cells, photodetectors, photovoltaic (PV) heterojunction structures and quantum well structures are well recognized [3]. ZnTe films were extensively studied for the applications as back contact material (p-type semiconductor) for CdTe in CdTe/CdS heterojunction solar cells [4-6]. The wide direct band gap makes ZnTe as one of the interesting materials for manufacturing of green light emitting diodes (LED) as well as other microelectronic and optoelectronic devices [7-9] including laser diodes and holographic interferometers.

Also, ZnTe exhibits unique electrical properties and high transparency in the infrared region which are very useful in infrared optoelectronics [10,11]. Because of its high electrooptic coefficient, ZnTe film is useful in the generation and detection of terahertz (THz) radiation [12] with application in imaging.

*Corresponding author: anca.cojocaru@chimie.upb.ro

Electrodeposition is among usual techniques used to prepare polycrystalline Zn_xTe_y films. It provides a simple, low-cost procedure for fabrication of thin-film semiconductors and allows the coating of large areas including surfaces with complicated profile [13]. Extensive work has been conducted for the electrodeposition of zinc telluride from acidic aqueous electrolytes with $ZnSO_4$ or $ZnCl_2$ as precursors for Zn species [14-18]. It has been found that the range of plating conditions leading to stoichiometric ZnTe is quite narrow compared to that given by thermodynamic calculation and the nobler component in the film is Te [19]. High bath temperatures are necessary for achieving fine microcrystalline films. Currently, a single-phase crystalline ZnTe films can be conveniently deposited by using citrate ion (citric acid and natrium citrate) as a complexing agent [19-22]. Citrate ion not only improves the solubility of Te^{4+} species due to the formation of complex species, but also favors the electrodeposition of polycrystalline ZnTe compound repressing the formation of Te phase. In addition, the pulse plating method was recommended, with simple periodic or more sophisticated profiles of pulses. Gromboni et al. [23] studied the multiple potentiostatic steps for electrodeposition of zinc telluride thin films using an acid aqueous solution ($ZnSO_4$, H_2SO_4, pH 0.3). The variation of initial polarization potential with values chosen from cyclic voltammograms enabled the selection of whether the first layer deposited was Te or Zn, respectively. The anodic peak is interpreted by the dissolution of a ZnTe phase formed during the cathodic scan by co-reduction of Te^{4+} and Zn^{2+}.

Unlike aqueous solutions, the use of electrolytes based on organic solvents [24,25] or high-temperature molten salts [26] avoids the problems related to low current efficiency due to hydrogen evolution which occurs simultaneously with ZnTe deposition. Organic baths containing ethylene glycol, methanol, acetonitrile and propylene carbonate were investigated at temperatures up to 150 ^oC [24,25]. The current efficiency was enhanced up to 60% in propylene carbonate where single-phase ZnTe was obtained working with a Zn^{2+}/Te^{4+} concentration ratio of 10 and Te^{4+} concentration between 0.1 mM to 0.2 mM $TeCl_4$. Studies describing the electrochemical synthesis of tellurides in traditional ionic liquids based on imidazolium or pyrrolidinium derivatives were carried out in recent years [27,28]. These media exhibit many advantages over other electrolytes because they are able to dissolve relatively high concentrations of tellurium precursor and the codeposition of Te with metal is easier. However, according our best knowledge there are no published studies, except a paper [29] regarding the ZnTe film preparation at 40^oC from a mixture of Lewis basic $ZnCl_2$ / 1-ethyl-3-methylimidazolium ($ZnCl_2$:EMIC) and 50%(w/w) propylene carbonate as a cosolvent. In this work $TeCl_4$ was the precursor for Te and oxyquinoline (8-quinolinol) was also added into the solution in order to shift the reduction of Te^{4+} to more negative potential, thus facilitating the codeposition of Zn and Te. Results from EDX elemental analysis confirmed stoichiometric ZnTe phase for the films prepared by constant potential electrolysis between -0.4 V and -0.65 V. Te-rich ZnTe deposit is obtained between -0.2 and -0.4 V, whereas Zn content in the deposit exceeds 50% at potentials more negative than -0.65 V.

However, in terms of technological application, the traditional ionic liquids come with some economical and potential toxicological and purity issues. Deep eutectic systems have very recently been considered as alternatives to classical room-temperature ionic liquids being water and air stable, nontoxic, cheap and able to dissolve relatively high concentrations of precursors [30]. Such analogous ionic liquids containing binary mixtures of choline chloride (*hydroxy-ethyl-trimethyl ammonium chloride*, ChCl) with ethylene glycol (EG) as hydrogen bond donor were used as the electrolytes to investigate the electrodeposition of metals and semiconductors. The Lewis-basic ChCl-EG (1:2 mole ratio) has commercial name Ethaline and already some studies on the electrodeposition of Zn pure metal have been conducted in this mixture [31-37].

In this work we investigated the electrode processes of co-reduction of Zn^{2+} and Te^{4+} ions in choline chloride – ethylene glycol ionic liquid in order to prepare zinc telluride films by electrodeposition. According to our best knowledge, the present study is a first work in deep eutectic systems media concerning the Zn and Te codeposition. Zinc telluride films electrodeposited on copper substrate were characterized by SEM microscopy, EDX analysis and X-ray diffraction.

2. Experimental Part

Ethaline as solvent was prepared by mixing choline chloride (Aldrich) with ethylene glycol (Aldrich) in 1:2 mole ratio and heating at 90°C for 30 min until a homogeneous colourless ionic liquid is formed. The liquid is stable at room temperature. The precursors of Zn^{2+} and Te^{4+} ions were anhydrous $ZnCl_2$ (Fluka) and TeO_2 (Alfa Aesar), respectively. By dissolving the precursors, the electrolyte with $ZnCl_2$+ TeO_2 remained colourless. A three-electrode cell containing a Pt sheet (0.5 cm^2) as working electrode, a large Pt plate as auxiliary electrode, and a Ag wire as quasi-reference electrode was used. Each measurement was carried out with cleaned Pt surface (polished with alumina paste, rinsed and dried) and freshly prepared electrolyte. A Bio-Logic SP150 potentiostat was employed for recording cyclic voltammograms (5-200 mVs^{-1}) and electrochemical impedance spectra (200 kHz – 50 mHz a.c. frequency and voltage amplitude of ±10 mV). All electrochemical investigations were carried out at constant temperature, 60 °C.

Zn_xTe_y films were electrodeposited on copper sheets in ChCl-EG based baths, without stirring, at 60 °C too. The cathodes were located vertically and had an exposed area of 4-8 cm^2; a parallel Pt sheet was used as anode in the cell and electrolyses in controlled potential conditions were conducted using the Bio-Logic SP150 potentiostat. After deposition for 0.5-3.5 hours the specimens were rinsed with water and acetone and air-dried. The as-deposited zinc telluride films grown by electrolysis without any further intentional heat treatment were then characterized. Scanning electron microscopy images were taken with a Zeiss EVO 50 XVP scanning electron microscope to show the morphology. The elemental composition was obtained by using energy-dispersive X-ray spectroscopy (EDX) with the same equipment. Also, X-ray diffraction (XRD) characterization regarding the crystalline phases of the films was done by using BRUKER D8-ADVANCE (from Bruker-AXS) with Cu anode at 40 kV, 40 mA (λ of Kα=1.5418 Å) and Lynx Eye unidimensional detector. BRUKER-EVA software was used for processing XRD data.

3. Results and Discussion

3.1. Electrochemical studies

First, an electrolyte containing only Zn^{2+} was examined at 60 °C by cyclic voltammetry (CV) on stationary Pt electrode at various scan rates, Fig. 1. A cathodic limiting current or a shoulder (for CVs at high scan rate) located at ca. -1.15 V and an associated anodic peak around -0.90 V can be observed. This couple which have not a classical nucleation loop at scan reversing would be interpreted as deposition of Zn metal and its stripping dissolution. Our data are similar with previous voltammograms recorded by different authors [33-36] in the ChCl-EG + $ZnCl_2$ ionic liquid systems. However, the small magnitude of stripping anodic peak as compared to the cathodic current shown in Fig. 1 may partly reflect the less complete dissolution of zinc previously deposited on Pt. This can suggest an irreversible behavior from electrochemical point of view of this couple, in spite of its diffusion control (mass transfer control). We suppose that the cathodic reaction is a two-electron transfer with Zn film formation:

$$Zn^{2+} + 2\,e \rightarrow Zn \qquad (1)$$

Certainly, the same cathodic process takes place if $ZnCl_4^{2-}$ chlorocomplex species [33,34] is supposed to exist in ionic liquid.

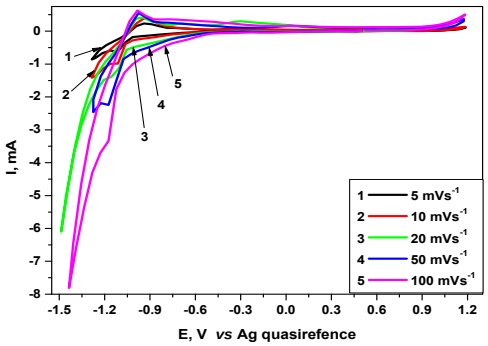

Fig. 1. CVs recorded at various scan rates on Pt in ChCl-EG + 15 mM $ZnCl_2$

In order to better understand the Zn film formation and its behavior, electrochemical impedance spectroscopy (EIS) plots were recorded in ChCl-EG + 15 mM $ZnCl_2$ at different polarization potentials in the range of the above discussed cathodic process. The corresponding Nyquist and Bode plots for progressive cathodic polarization are shown in Figures 2a-c. The diameter represents the charge transfer resistance which is inversely proportional to the electrolysis current. Another parameter of interest is the maximum phase angle.

It can be seen that the corresponding Nyquist semicircles and Bode curves for impedance modulus and for phase angle up to -1 V polarization are almost superposed. These may be correlated with Zn underpotential deposition as some waves observed on voltammograms in the first portion after starting the scan. However, the shape and diameter of semicircle in Nyquist diagram (Fig. 2a) are drastically modified by polarizing the Pt electrode at -1 V where the smallest diameter (corresponding to the largest electrolysis current) indicates a massive (bulk) deposition of Zn. Moreover, the semicircle is followed at low frequencies by several experimental points along a straight line which is characteristic for a film formation. It can be seen that Bode plots for this polarization indicate the lowest curve of impedance modulus (Fig. 2b) and the lowest maximum phase angle; value of -18° in Fig. 2c is typically for good electrical conduction of a metallic film.

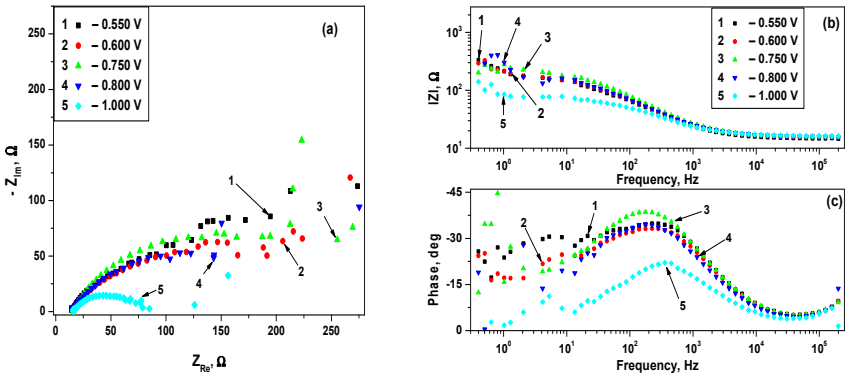

Fig. 2. Nyquist (a) and Bode (b,c) plots on Pt in ChCl-EG +15 mM $ZnCl_2$, at different polarization potentials

The electrochemical behavior of Pt at 60 °C in Ethaline containing both Zn^{2+} and Te^{4+} was first examined by cyclic voltammetry. CV curves were recorded at 5-50 mVs^{-1} for different Zn^{2+} over Te^{4+} concentration ratios (Figs. 3a-d). In order to evidence the processes of Te^{4+} ions, preliminary CV curves were obtained (not shown here) from ChCl-EG ionic liquids with 5-10 mM single dissolved TeO_2. A cathodic peak assigned to the massive (bulk) Te deposition was identified at *ca.* -0.55 V, after a large plateau of current from 0.3 V to -0.3 V attributed to Te underpotential deposition, Te-UPD. Anodic branches of those CV curves exhibited two successive

peaks; the first at 0.1 V was associated to dissolution of film previously deposited as bulk Te, and the second at 0.6 V due to stripping from platinum of Te monolayer formed incompletely during Te-UPD process.

In the examples illustrated by Figures 3, during the first portion of scanning Te element is underpotentially deposited onto substrate surface. A current plateau or small waves of Te-UPD occur at potentials up to -0.3 V attributed to a four-electron transfer, as literature of traditional ionic liquids based on imidazolium has mentioned [38,39]:

$$Te^{4+} + 4\,e^- \rightarrow Te \qquad (2)$$

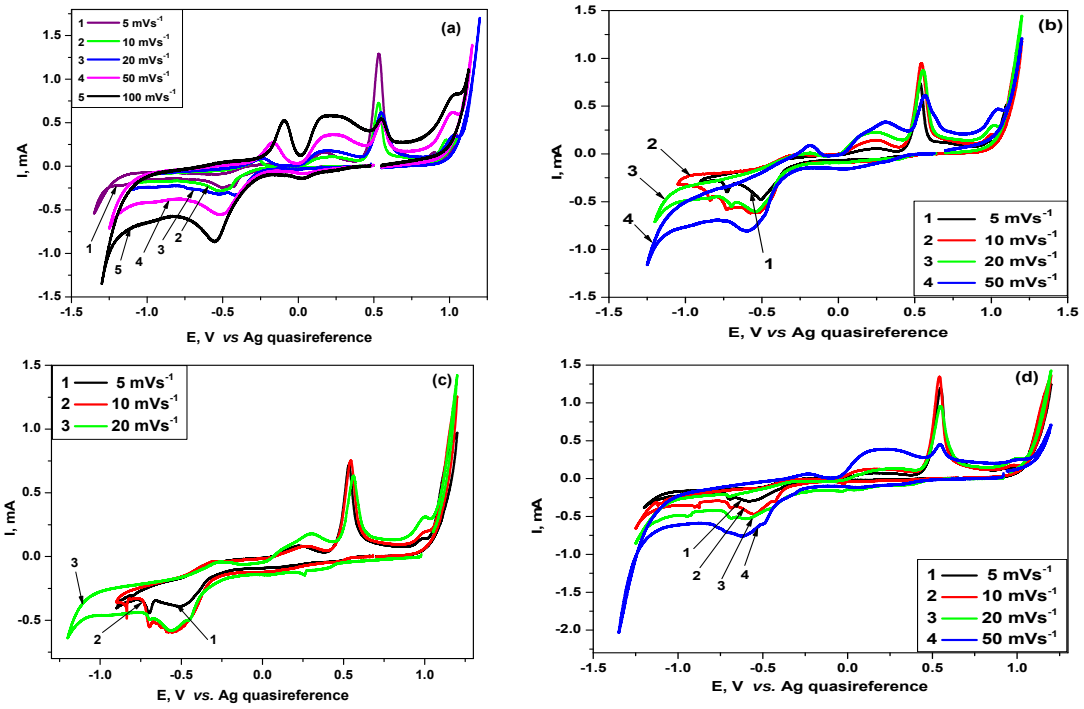

Fig. 3. CVs recorded at various scan rates on Pt from ChCl-EG ionic liquid with different precursors concentrations: (a) 24 mM $ZnCl_2$ + 8 mM TeO_2; (b) 20 mM $ZnCl_2$ + 10 mM TeO_2; (c) 10 mM $ZnCl_2$ + 10 mM TeO_2; (d) 5 mM $ZnCl_2$ + 8 mM TeO_2

In contrast to the voltammograms from single Zn deposition shown in Fig. 1, the main cathodic peak recorded in ChCl-EG + $ZnCl_2$ + TeO_2 is located at more positive potentials, between -0.45 and -0.65 V. It may be attributed to the massive deposition of tellurium, described by the equation (2). Its peak current increases with square root of scan rate suggesting a mass transfer (diffusion) control. If the potential is scanned more negative, two processes of co-reduction of Zn^{2+} ions are expected, either the direct co-reduction of both ions, Zn^{2+} and Te^{4+}:

$$Zn^{2+} + Te^{4+} + 6\,e^- \rightarrow ZnTe \qquad (3)$$

or co-reduction of Zn^{2+} with Te ad-atoms already produced by the process (2) during Te-UPD:

$$Zn^{2+} + Te + 2\,e^- \rightarrow ZnTe \qquad (4)$$

These processes are not well evidenced on voltammograms in the ionic liquid richer in Zn^{2+} (Fig. 3a) where only some small waves can be observed at slow scan rates. However, they are well illustrated at slow scans in Figures 3b-d as a unique reduction peak at about -0.7 V or two successive peaks at -0.7 V and -0.85 V, suggesting an overlay or separation of processes (3) and (4). Because Zn and Te elements are not soluble into each other to form a solid solution, the only

formed phase is the semiconductor zinc telluride compound with 1:1 stoichiometry [1,2]. Comparing to the deposition of pure Zn from ChCl-EG + $ZnCl_2$ the potential at ZnTe deposition is with 400 mV more positive, explained because Te is the nobler component in ZnTe film. In an extension of potential scanning to more negative than -1 V, the bulk deposition of Zn metal (process (1)) is produced as a continuous increase of current on CV curves. This leads therefore to an increase in the zinc content of deposited film.

Successive distinct processes are noticed on the anodic branches of CVs in Figures 3. The first process after reversing the scan is assigned to the electrochemical dissolution of Zn freshly deposited cathodically. In Figs. 3a,b this is illustrated by a clear peak at about -0.25 V, which shifts its potential toward positive for increasing scan rate. For systems with lower content in Zn^{2+} a broad peak with small amplitude can be observed in the same potential region (Figs. 3c,d). The second anodic peak is a broad peak (centred at around 0.3 V) which represents in fact an overlay of two dissolution processes, of ZnTe compound and of bulk deposited Te. The third peak (at 0.6 V) which is very sharp was attributed to stripping dissolution from Pt of tellurium monolayer deposited during UPD process. It is worth to mention that the first two anodic peaks increase in their currents with scan rate. The current of the third anodic peak decreases gradually with scan rate, thus confirming Te formation by UPD. At the end of anodic scan, at very positive potentials (*ca.* 1.1 V), CV curves in Figures 3 show an oxidation peak assigned to the oxidation of Cl^- ions from Ethaline.

Further, in order to get detailed information about the electrode processes, EIS measurements were performed in the same Ethaline + $ZnCl_2$ + TeO_2 ionic liquids and the corresponding Nyquist and Bode plots are shown in Figures 4-7. Different polarization potentials were selected in the ranges where the massive deposition of Te, co-reduction of Zn^{2+} with Te^{4+} and deposition of Zn are expected to take place successively. The changes with electrode potential of the Nyquist semicircle shape and diameter are interpreted in relation with voltammetric results.

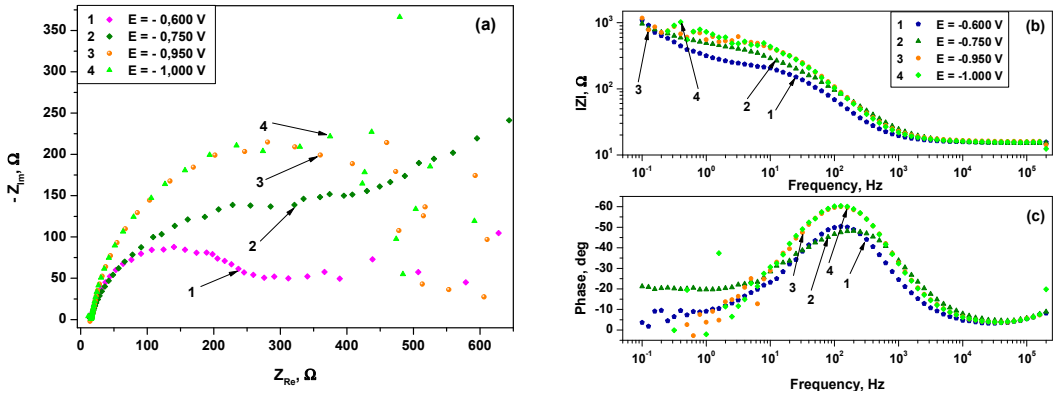

Fig. 4. Nyquist (a) and Bode (b,c) plots on Pt at various polarization potentials from ChCl-EG + 24 mM $ZnCl_2$ + 8 mM TeO_2

All semicircles recorded for potentials between -0.5 and -0.7 V have diameters of 75-100 Ωcm^2 and are followed by straight lines in the region of low frequencies. They suggest the existence of massive deposition of tellurium. Te film is a semiconductor [40,41] which passivate the Pt surface. As a consequence the electrolysis current decreases and values between -38° and -48° for the maximum phase angle in Bode diagrams were observed. More cathodic polarization of the electrode, from -0.75 to -0.85 V, has led to an increase in diameter for Nyquist semicircles, up to 200 Ωcm^2 (Fig. 4a), owing to ZnTe phase formation by processes (3) and (4). It seems that this semiconductor compound has a lower conduction than Te element [42-44] therefore the charge-transfer resistance increases. Also, the maximum phase angle of ZnTe grown from all solutions has values between -43° and -53° and its different values may be explained by different thickness and compactness of films.

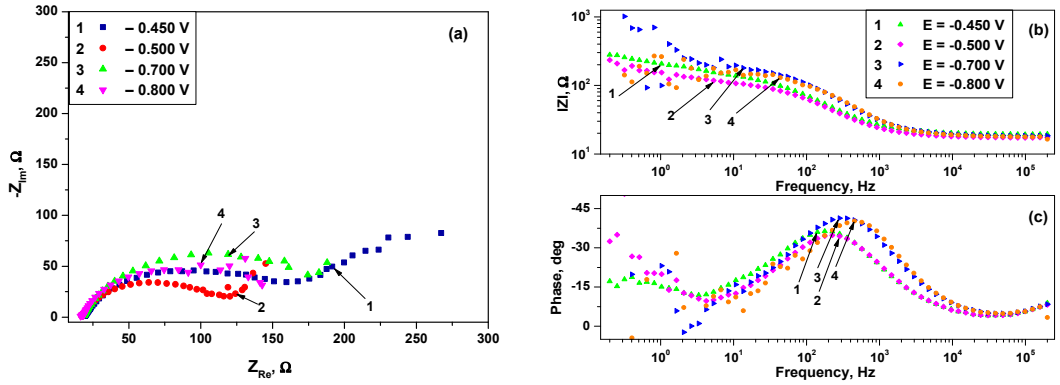

Fig. 5. Nyquist (a) and Bode (b,c) plots recorded on Pt at various polarization potentials from ChCl-EG + 20 mM $ZnCl_2$ + 10 mM TeO_2 ionic liquid

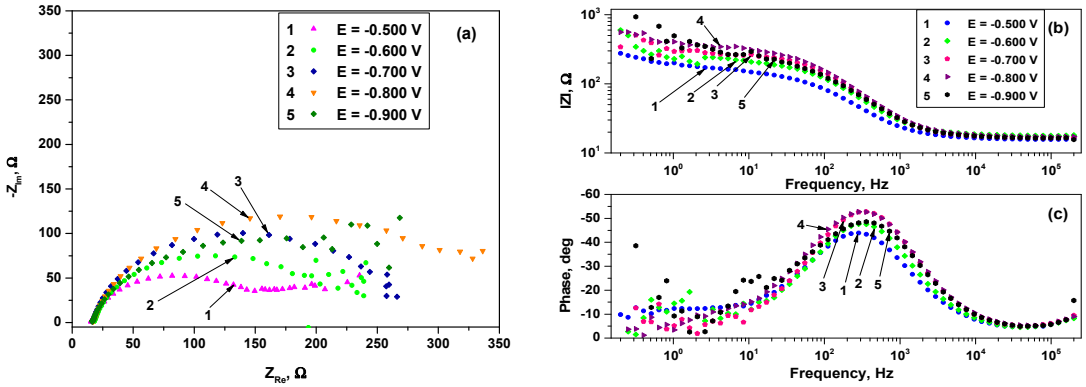

Fig. 6. Nyquist (a) and Bode (b,c) plots recorded on Pt at various polarization potentials from ChCl-EG + 10 mM $ZnCl_2$ + 10 mM TeO_2 ionic liquid

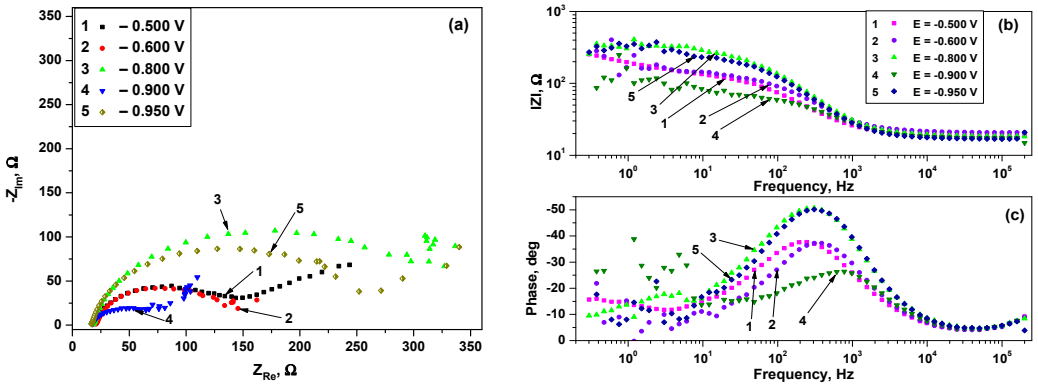

Fig. 7. Nyquist (a) and Bode (b,c) plots recorded on Pt at various polarization potentials from ChCl-EG + 5 mM $ZnCl_2$ + 8 mM TeO_2 ionic liquid

For polarization at excessive negative potentials (more than -0.9 V), Zn layers are expected to be formed onto ZnTe semiconductor and this process should lead to a decrease in Nyquist semicircle diameter, as Figs. 5a and 7a show. Also, the maximum phase angle should decrease (Figs. 5c and 6c) reaching even -25° for the case of 5 mM Zn^{2+} + 8 mM Te^{4+} (Fig. 7c).

However, these did not happen for Zn film grown from the bath with 24 mM Zn^{2+} + 8 mM Te^{4+} (Figs. 4) where both semicircle diameter and maximum phase angle increased at -1.0 V polarization. An explanation may be a rapid thickening followed by an oxidation of metallic film which is partially converted into zinc oxide.

3.2. Preparation and characterization of zinc telluride films

Zinc telluride films were deposited on Cu substrate by constant potential electrolysis from the choline chloride – ethylene glycol mixture (Ethaline) with different compositions in Zn^{2+} and Te^{4+}, at 60 ^{o}C.

Table 1. Chemical composition determined by EDX analysis and apparent stoichiometry of some Zn_xTe_y films electrodeposited at 60 ^{o}C from Ethaline + $ZnCl_2$ + TeO_2 ionic liquids

Samples (apparent stoichiometry)	**Electrolysis conditions and elemental composition of deposited films**			
	wt% Zn (mean values)	**wt% Te** (mean values)	**at% Zn** (mean values)	**at% Te** (mean values)
A* (**$Zn_{14.11}Te$**)	ChCl-EG + 24 mM $ZnCl_2$ + 8 mM TeO_2, 3.5 h, at -1.35 V			
	81.10	11.22	68.59	4.86
B (**$Zn_{1.60}Te$**)	ChCl-EG + 15 mM $ZnCl_2$ + 10 mM TeO_2, 0.5 h, at -1.35 V			
	45.08	54.92	61.57	38.43
C (**ZnTe**, exactly **$Zn_{1.07}Te$**)	ChCl-EG + 15 mM $ZnCl_2$ + 10 mM TeO_2, 1 h, at -1.25 V			
	35.37	64.63	51.64	48.36
D** (**$Zn_{0.65}Te$**)	ChCl-EG + 15 mM $ZnCl_2$ + 10 mM TeO_2, 0.5 h, at -1.0 V			
	16.73	50.15	9.58	14.80

*The film **A** contains additional 7.68 wt% O (26.54 at% O) which may come from oxidation of deposited Zn;

The film **D also contains 20.29 wt% O +12.83 wt% C (42.47 at% O + 35.80 at% C); in this case, both oxygen and carbon species likely originate from ionic liquid that was not fully removed from the surface.

The obtained Zn_xTe_y films in non-annealed state were then characterized in terms of morphology, composition and microstructure by SEM microscopy/EDX analysis and XRD. Table 1 presents the results of EDX elemental analysis for some electrodeposits.

As Table 1 shows, zinc content in the sample A is in a great excess in comparison to tellurium, and this may be due to the large content of zinc ions in electrolyte and also due to -1.35 V polarization which favors zinc deposition. The atomic percentage of zinc in the deposit decreases if the Zn^{2+} concentration in the electrolyte decreases. The effect of cathodic polarization on the zinc content in the deposits may be evidenced by a comparison of samples B-D obtained from the same electrolyte, Ethaline + 15 mM Zn^{2+} + 10 mM Te^{4+} at 60 ^{o}C. The target composition ZnTe (1:1 stoichiometry) of films was achieved in this ionic liquid only by performing electrolysis right at -1.25 V polarizations. As shown above, on all cyclic voltammetry curves in Figs. 3 this potential is located after (*i.e.* more negative) the potential range where ZnTe is supposed to be co-deposited. Because our samples were not annealed, this means that the amount of Zn metal formed onto ZnTe layer at -1.25 V has balanced all Te amount deposited before ZnTe compound.

Working with the same bath, Ethaline + 15 mM $ZnCl_2$ + 10 mM TeO_2, the percentage of zinc obtained at potentials very negative (*e.g.* -1.35 V, sample B) surpasses that of tellurium, whereas at potentials more positive than -1.25 V the Zn content becomes lower, being already *ca.* 2/3 from Te content at -1.0 V polarization (sample D). Thus, EDX results confirm the predominant Zn deposition when the current starts increasing in the final portion on voltammograms and predominant Te deposition together with ZnTe if the electrolysis is performed at controlled potential between -0.75 and -1.0 V, regardless of Zn^{2+} content into the electrolyte.

Actually, we have not reached experimentally the exact ZnTe composition, but $Zn_{1.07}Te$ (sample C) is the closest to the desired 1:1 ratio. Therefore, we could indicate exactly the important parameters of electrolysis (bath composition, electrodeposition potential) for obtaining 1:1 stoichiometry of zinc telluride film without post-treatment of annealing. In spite of studies in

aqueous electrolytes that recommend a large excess of Zn^{2+} concentration over the Te^{4+} concentration in the solution [19-22,25], our results in Ethaline ionic liquid demonstrate that this ratio would decrease even to 1.5 value. Unfortunately, polycrystalline Zn_xTe_y films of nearly stoichiometric composition can be obtained by applying a potential in a narrow range, probably between -1.1 and -1.3 V vs. Ag quasi-reference. A systematic investigation needs to be undertaken in the future, including the influence of temperature.

The morphology of Zn_xTe_y films grown at 60 ^oC without any heat treatment was also found to depend on the plating conditions and is interpreted according to EDX compositional analysis (Table 1). The SEM pictures of some as-deposited films are shown in Figures 8. Figs. 8a,a' show uniform and fine metallic Zn grains electrodeposited on copper substrate from Ethaline + 24 mM $ZnCl_2$ + 8 mM TeO_2 at -1.35 V polarization. Only few ZnTe crystallites as aggregates with cauliflower-like shape can be seen on the surface of the film A. Their number increases for the same polarization by changing the Zn^{2+} to Te^{4+} concentration ratio in the second electrolyte (Ethaline + 15 mM $ZnCl_2$ + 10 mM TeO_2). Thus, in the micrographs of sample B (Figs. 8b,b') obtained at the same potential as sample A, a part of the aggregates appears somewhat as coalescent microcrystals.

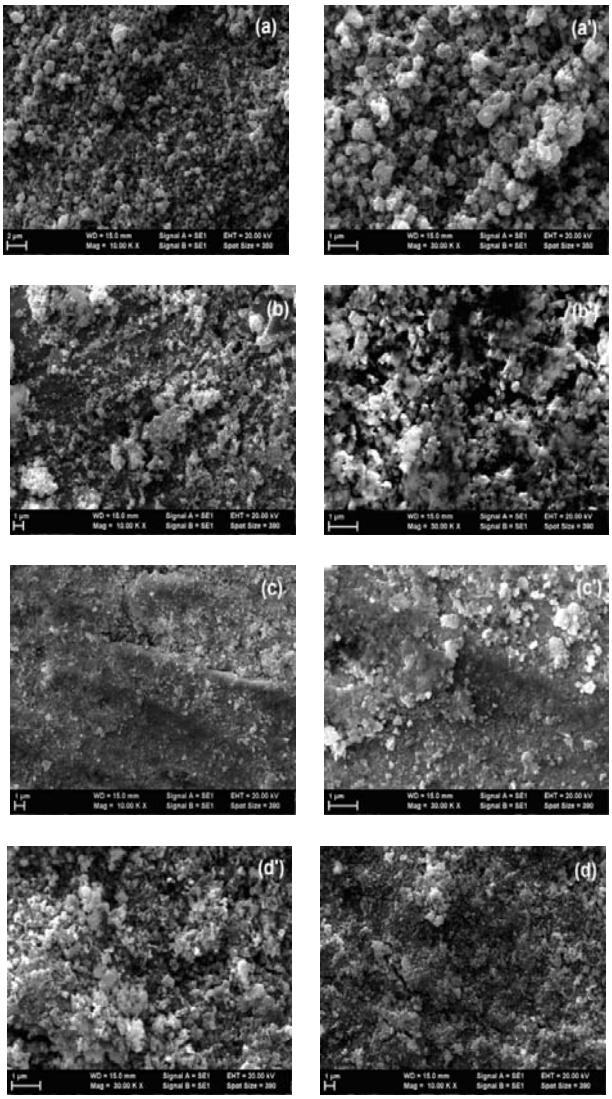

Fig. 8. SEM micrographs at two magnifications (× 10000 and × 30000) for some as-grown zinc telluride films (see Table 1): (a,a') sample A; (b,b') sample B; (c,c') sample C; (d,d') sample D

The aspect of dense ZnTe particles becomes predominantly if the polarization during electrolysis is more positive than -1.35 V (-1.25 V, sample C for instance). SEM images in Figs. 8c,c' reveal a dense and coherent ZnTe deposit with a grain size homogeneity, although its thickness is not uniform. The last micrographs (Figs. 8d,d') taken for film D grown by electrolysis at -1.0 V in the same ionic liquid show that this polarization does not favor metallic Zn deposition. Therefore, the resulting growth has led, together with ZnTe aggregates, to an amount of elemental Te as needle-like crystallites, randomly oriented.

XRD measurements provide insight into the phase composition of the as-deposited Zn_xTe_y films. For comparison purposes, we additionally have prepared and XRD analysed two new films from Ethaline + $ZnCl_2$ + TeO_2 ionic liquids at 60°C with higher concentration of Te^{4+} in the electrolysis bath. All selected XRD patterns presented in Figures 9 exhibit multi-phase nature of the obtained films. They show the characteristic peaks of both cubic ZnTe (denoted ZnTe c) and hexagonal ZnTe (ZnTe h). It can be seen that the relative intensities between these peaks changed as a function of the bath composition and applied potential and some peaks are shifted from the standard 2θ positions. ZnTe c may belong to two spatial groups, either F-43m (zinc blende type) or Fm-3m and occurs clearly in Fig. 9a at 25.5° (111) and 41.9° (220), as well as in Fig. 9b at 25.5° (111). Peaks for ZnTe h phase occur in Fig. 9a at 35.3° (102), 46° (103) and 49° (201). In Fig. 9b the peaks of this phase occur at 46° (103) and 49° (201). Peaks for copper substrate as well as for elemental Te were also found in the diffractograms. Peaks for hexagonal Te can be observed at 23°, 27.8°, 38.5°, 41° and 43.5°, and they fit well with the corresponding ICDD reference data.

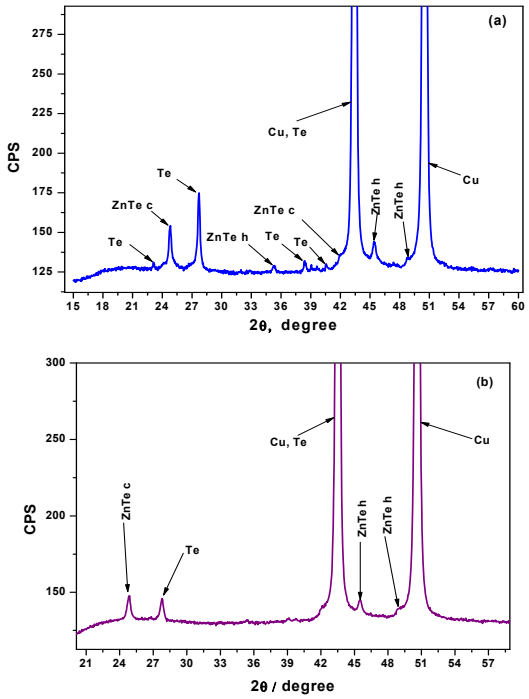

Fig. 9. XRD patterns for Zn_xTe_y films electrodeposited on Cu substrate at 60 °C from Ethaline ionic liquid with various precursors concentrations and electrolysis parameters: (a) 32 mM $ZnCl_2$ + 8 mM TeO_2, 1.5 h, at -0.80 V; (b) 25 mM $ZnCl_2$ + 10 mM TeO_2, 1.5 h, at -0.80 V;

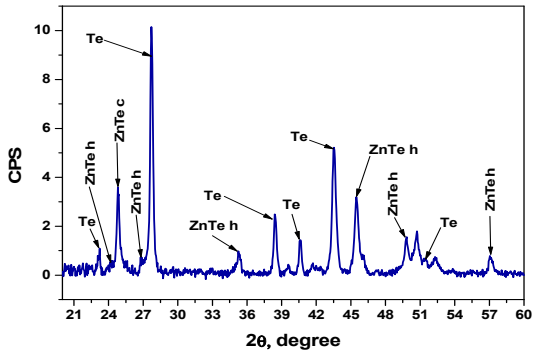

Fig. 10. XRD pattern for Zn_xTe_y powder prepared at 60 °C, from Ethaline + 32 mM $ZnCl_2$ + 8 mM TeO_2, 1.5 h, at -0.80 V. This sample was detached from the substrate and powdered

As XRD pattern in Fig. 10 shows the two peaks for copper are not present, as expected. Peaks for cubic ZnTe occur only at 25.0° (111) and for hexagonal ZnTe they are located at 24.0° (002), 27.2° (101), 35.3° (102), 46.0° (103), 49.2° (201) and 57.0° (shifted from 56.2° standard value). Peaks for hexagonal Te occur at 23.2°, 27.8°, 38.5° and 52.2°.

All results from XRD analysis confirm the above data and interpretations from cyclic voltammetry, electrochemical impedance spectroscopy and SEM/EDX analysis. It seems that the main parameter to be controlled during electrolysis is the applied electrode potential. Thus, XRD patterns in Figs. 9 and 10 demonstrate that Zn_xTe_y films with Te-rich composition may be prepared from electrolytes based on Ethaline with Zn^{2+} : Te^{4+} ion concentration ratio up to 4 if the polarization is more positive than -1 V.

4. Conclusions

The cathodic processes on platinum at 60 °C in Ethaline containing Zn^{2+} and Te^{4+} were examined in details by cyclic voltammetry and electrochemical impedance spectroscopy. The electrode processes shown in CV curves consist in successive depositions of Te element, ZnTe stoichiometric compound and metallic Zn. The anodic behavior shows the reverse order of electrochemical dissolution of layers. The impedance investigation revealed the effects of both concentration of precursors in electrolyte and gradual cathodic polarization upon the charge transfer resistance (that is inverse proportional with the electrolysis current) as well as upon the semiconductor character of the deposit.

EDX elemental analyses for films grown on copper substrate at 60 °C confirmed the possible deposition of ZnTe with 1:1 stoichiometry at controlled potential in Ethaline + $ZnCl_2$ + TeO_2 bath. Unfortunately, the range of applied potentials for obtaining exactly ZnTe composition is found to be quite narrow and therefore preliminary electrochemical studies are very useful. Phases of ZnTe, Te and Zn are exactly balanced within ZnTe stoichiometric deposit. Tellurium is the nobler component, whereas zinc is deposited in excess at very negative potentials. Thus, the different morphology of films showed by SEM micrographs may be explained.

XRD studies revealed that Zn_xTe_y films are crystalline in nature. The diffraction patterns exhibit both cubic and hexagonal structures of ZnTe semiconductor compound. In general, locations of XRD peaks for ZnTe and Te phases have fitted well with ICDD reference data.

Acknowledgements

The authors wish to thank PhD researcher Iuliana Pasuk (National Institute of Materials Physics, Romania) for providing XRD patterns and their interpretation. One of the authors (A.-S.

Catrangiu) recognizes support from the European Social Fund through POSDRU / 132395/Inno Research Project.

References

[1] R. C. Sharma, Y. A. Chang, Bull. Alloy Phase Diagr. **8**(1), 14 (1987).
[2] Y. Feutelais, A. Haloui, B. Legendre, J. Phase Equilibria **18**(1), 48 (1997).
[3] T. Mahalingam, V.S. John, P.J. Sebastian, J. Physics: Condensed Matter. **14**(21), 5367 (2002).
[4] K. R. Murali, M. Ziaudeen, N. Jayaprakash, Solid State Electron. **50**, 1692 (2006).
[5] G. H. Tariq, N. A. Niaz, M. Anis-ur-Rehman, Chalcog. Lett. **11**(9), 461 (2014).
[6] O. Toma, S. Antohe, Chalcog. Lett. **11**, 611 (2014).
[7] G. Lastra, M. A. Quevedo-Lopez, A. Olivas, Chalcog. Lett. **11**, 67 (2014).
[8] B. Rajesh Kumar, B. Hymavathi, T. Subba Rao, Chalcog. Lett. **11**, 509 (2014).
[9] W. A. Syed, S. Ahmed, M. S. Saleem, N. A. Shah, Chalcog. Lett. **12**(5), 215 (2015).
[10] M. S. Hossain, R. Islam, K. A. Khan, Chalcog. Lett. **5**, 1 (2008).
[11] M. S. Hossain, R. Islam, K. A. Khan, Chalcog. Lett. **7**, 21 (2010).
[12] M. Walther, M. R. Freeman, F. A. Hegmann, Appl. Phys. Lett. **87**(26), 261107 (2005).
[13] A. E. Rakhshani, Semicond. Sci. Technol. **19**, 543 (2004).
[14] B. Bozzini, A. Baker, P. L. Cavallotti, E. Cerri, C. Lenardi, Thin Solid Films **361–362**, 388 (2000).
[15] D. H. Han, S. J. Choi, S. M. Park, J. Electrochem. Soc. **150**, C342 (2003).
[16] D. G. Diso, F. Fauzi, O. K. Echendu, A. R. Weerasinghe, I. M. Dharmadasa, J. Phys.: Conference Ser. **286**, 012040 (2011).
[17] T. Mahalingam, V. Dhanasekaran, K. Sundaram, A. Kathalingam, J. K. Rhee, Ionics **18**, 299 (2012).
[18] F. Fauzi, D. G. Diso, O. K. Echendu, V. Patel, Y. Purandare, R. Burton, I. M. Dharmadasa, Semicond. Sci. Technol. **28,** 045005 (2013).
[19] M. Bouroushian, T. Kosanovic, D. Karoussos, N. Spyrellis, Electrochim. Acta **54**, 2522 (2009).
[20] T. Ishizaki, T. Ohtomo, A. Fuwa, J. Electrochem. Soc. **151**, C161 (2004).
[21] T. Ishizaki, N. Saito, O. Takai, S. Asakura, K. Goto, A. Fuwa, Electrochim. Acta **50**, 3509 (2005).
[22] E. Beltowska-Lehman, P. Ozga, Arch. Metall. Mater. **50**, 319 (2005).
[23] M. F. Gromboni, F. W. S. Lucas, L. H. Mascaro, J. Braz. Chem. Soc. **25**(3), 526 (2014).
[24] N. B. Chaure, R. Jayakrishnan, J. P. Nair, R. K. Pandey, Semicond. Sci. Technol. **12**, 1171 (1997).
[25] P. Heo, R. Ichino, M. Okido, Electrochim. Acta **51**, 6325 (2006).
[26] K. Kuroda, T. Kobayashi, T. Sakamoto, R. Ichino, M. Okido, Thin Solid Films **478**, 223 (2005).
[27] N. Borisenko, S. Zein El Abedin, F. Endres, Chapter 6. Electrodeposition of Semiconductors in Ionic Liquids, in: Electrodeposition from Ionic Liquids, F. Endres, A.P. Abbott, D.R. MacFarlane, Eds, Wiley-WCH, Weinheim, 147 (2008).
[28] N. Borisenko, Chapter 12. Electrodeposition of Semiconductor in Ionic Liquids, in Electrochemistry in Ionic liquids, Vol. 2 Applications, A. A. J. Torriero, Ed., Springer Int. Publ. Switzerland, London, 359 (2015).
[29] M. C. Lin, P. Y. Chen, I. W. Sun, J. Electrochem. Soc. **148**(10), C653 (2001).
[30] Q. Zhang, K. De Oliveira Vigier, S. Royer, F. Jerome, Chem. Soc. Rev. **41**, 7108 (2012).
[31] F. Endres, S. Zein El Abedin, Q. Liu, D. R. MacFarlane, K. S. Ryder, A. P. Abbott, Electrodeposition of Zinc Coatings from a Choline Chloride: Ethylene Glycol-Based Deep Eutectic Solvent, Chapter 12. Plating Protocols, in: Electrodeposition from Ionic Liquids, F. Endres, A.P. Abbott, D.R. MacFarlane, Eds, Wiley-WCH, Weinheim, 365 (2008).
[32] A. P. Abbott, J. C. Barron, K. S. Ryder, Trans. Inst. Met. Finish. **87**(4), 201 (2009).

[33] A. H. Whitehead, M. Pölzler, B. Gollas, J. Electrochem. Soc. **157**(6), D328 (2010).
[34] A. P. Abbott, J. C. Barron, G. Frisch, K. S. Ryder, A. F. Silva, Electrochim. Acta **56**, 5272 (2011).
[35] N. M. Pereira, P. M. V. Fernandes, C. M. Pereira, A. F. Silva, J. Electrochem. Soc. **159**(9), D501 (2012).
[36] L. Vieira, A. H. Whitehead, B. Gollas, J. Electrochem. Soc. **161**(1), D7 (2013).
[37] M. Starykevich, A. N. Salak, D. K. Ivanou, A. D. Lisenkov, M. L. Zheludkevich, M. G. S. Ferreira, Electrochim. Acta **170**, 284 (2015).
[38] J. Szymczak, S. Legeai, S. Diliberto, S. Migot, N. Stein, C. Boulanger, G. Chatel, M. Draye, Electrochem. Commun. **24**, 57 (2012).
[39] R. W. Tsai, Y. T. Hsieh, P. Y. Chen, I. W. Sun, Electrochim. Acta **137**, 49 (2014).
[40] M. Rusu, J. Optoelectr. Adv. Mater. **3**(4), 867 (2001).
[41] M. H. Suhail, S. G. Kaleel, M. R. Fahad, Int. Res. J. Eng. Sci. Technol. Innov. **1**(5), 122 (2012).
[42] T. Ishizaki, T. Ohtomo, J. Phys. D: Appl. Phys. **37** (2) 255 (2004).
[43] E. Bacaksiz, S. Aksu, N. Ozer, M. Tomakin, A. Ozcelik, Appl. Surf. Sci. **256,** 1566 (2009).
[44] J. Pattar, S. N. Sawant, M. Nagaraja, N. Shashank, K. M. Bala Krishna, G. Sanjeev, H. M. Mahesh, Int. J. Electrochem. Sci. **4**, 369 (2009).